

# SCIENTIFIC REPORTS



OPEN

## A Redox-Nucleophilic Dual-Reactable Probe for Highly Selective and Sensitive Detection of H<sub>2</sub>S: Synthesis, Spectra and Bioimaging

Received: 13 May 2016

Accepted: 27 June 2016

Published: 21 July 2016

Changyu Zhang<sup>1</sup>, Runyu Wang<sup>2,3</sup>, Longhuai Cheng<sup>2,3</sup>, Bingjie Li<sup>1</sup>, Zhen Xi<sup>2,3</sup> & Long Yi<sup>1</sup>

Hydrogen sulfide (H<sub>2</sub>S) is an important signalling molecule with multiple biological functions. The reported H<sub>2</sub>S fluorescent probes are majorly based on redox or nucleophilic reactions. The combination usage of both redox and nucleophilic reactions could improve the probe's selectivity, sensitivity and stability. Herein we report a new dual-reactable probe with yellow turn-on fluorescence for H<sub>2</sub>S detection. The sensing mechanism of the dual-reactable probe was based on thiolysis of NBD (7-nitro-1,2,3-benzoxadiazole) amine (a nucleophilic reaction) and reduction of azide to amine (a redox reaction). Compared with its corresponding single-reactable probes, the dual-reactable probe has higher selectivity and fluorescence turn-on fold with magnitude of multiplication from that of each single-reactable probe. The highly selective and sensitive properties enabled the dual-reactable probe as a useful tool for efficiently sensing H<sub>2</sub>S in aqueous buffer and in living cells.

Hydrogen sulfide (H<sub>2</sub>S) is an important endogenous signalling molecule with multiple biological functions<sup>1–7</sup>. H<sub>2</sub>S could be enzymatically produced by three distinctive pathways including cystathionine β-synthase (CBS), cystathionine γ-lyase (CSE) and 3-mercaptopyruvate sulfurtransferase (3-MPST)/cysteine aminotransferase (CAT) in different organs and tissues<sup>3,4</sup>. Studies have shown that the H<sub>2</sub>S level *in vivo* is correlated with numerous diseases, including the symptoms of Alzheimer's disease, Down syndrome, diabetes and liver cirrhosis<sup>1,8</sup>. Despite H<sub>2</sub>S has been recognized to be linked to numerous physiological and pathological processes, many of its underlying molecular events *in vivo* remain largely unknown. Therefore, it presents significant research value to develop efficient methods for detection of H<sub>2</sub>S in living biological systems.

Compared with traditional methods<sup>9–12</sup>, fluorescent probes should be excellent tools for *in situ* monitoring H<sub>2</sub>S in biological samples because of their non-destructive sensing of bio-targets with readily available detection<sup>13–42</sup>. Organic reactions including H<sub>2</sub>S-mediated reduction<sup>14–28</sup>, nucleophilic addition/substitution<sup>29–33</sup>, and dual-nucleophilic addition/substitution<sup>34–39</sup> were employed for development of H<sub>2</sub>S fluorescent probes. Though the great success of these fluorescent probes, we still need to develop probes with higher selectivity and sensitivity for detection of biological H<sub>2</sub>S in living systems. We have proposed a dual-reactive and dual-quenching strategy for improvement of probe's selectivity and sensitivity, respectively<sup>40–42</sup>. However, the combination usage of both redox reaction and nucleophilic reaction for H<sub>2</sub>S probes was rarely explored<sup>42</sup>. Furthermore, in our previous work for dual-reactable probes<sup>40–42</sup>, we did not prepare “exact” control probes (single-reactable probes with the same fluorophore and reaction group as that of the dual-reactable probe) for comparable studies, which was insufficient for understanding the properties of dual-reactable probes. Herein, we report a dual-reactable probe **1** based on 1,8-naphthalimide as fluorophore (Fig. 1) for highly selective and sensitive detection of H<sub>2</sub>S in living cells. The two single-reactable control probes **2** and **3** were also prepared, which revealed that the improved

<sup>1</sup>State Key Laboratory of Organic-Inorganic Composites, Beijing University of Chemical Technology (BUCT), Beijing, China. <sup>2</sup>State Key Laboratory of Elemento-Organic Chemistry, Department of Chemical Biology, National Engineering Research Center of Pesticide (Tianjin), Nankai University, Tianjin, China. <sup>3</sup>Collaborative Innovation Center of Chemical Science and Engineering, Nankai University, Tianjin, China. Correspondence and requests for materials should be addressed to Z.X. (email: zhenxi@nankai.edu.cn) or L.Y. (email: yilong@mail.buct.edu.cn)

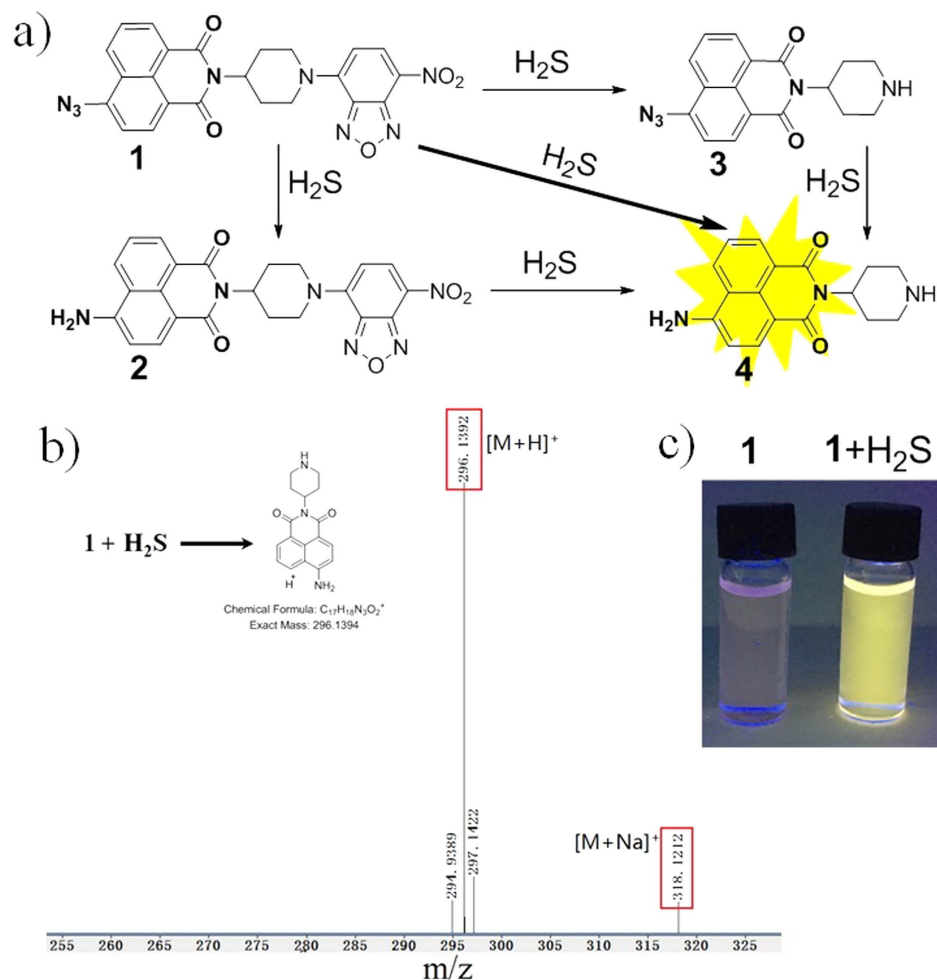


**Figure 1.** Reaction of the dual-reactable probe toward H<sub>2</sub>S. (a) Structure of a dual-reactable probe 1 and its reaction with H<sub>2</sub>S to give single-reactable probes 2 and 3 and the fluorophore 4. (b) High resolution mass spectrum for the reaction solution of probe 1 and H<sub>2</sub>S revealed the production of 4. (c) Photo of probe 1 and its reaction with H<sub>2</sub>S under 365 nm UV lamp.

turn-on fold and selectivity of the dual-reactable probe could be magnitude of multiplication from that of the two single-reactable probes 2 and 3.

## Results and Discussion

To obtain H<sub>2</sub>S fluorescent probes with higher selectivity, we decided to develop dual-reactable H<sub>2</sub>S probes based on both redox and nucleophilic reactions. However, our previous probes were based on multi-step organic synthesis and coumarin fluorophores with relatively short emission<sup>42</sup>. The reduction of aromatic azide to amine is the most used redox reaction for H<sub>2</sub>S probe<sup>13–24</sup>. The nucleophilic reaction of thiolysis of NBD (7-nitro-1,2,3-benzoxadiazole) amine have been explored by us to develop H<sub>2</sub>S probes<sup>31</sup>. In this work, we used the reduction of aromatic azide and thiolysis of NBD amine for development of a new dual-reactable fluorescence probe 1. The synthesis of 1 is straightforward from commercially available reagents. Moreover, both NBD and azide moieties could quench fluorescence of the naphthalimide fluorophore in 1 through fluorescence resonance energy transfer (FRET) and intramolecular charge transfer (ICT) effects, respectively.

The synthesis of 1 was achieved by coupling reaction of single-reactable probe 3 and NBD-Cl. Probe 3 was prepared from commercially available reagents 4-bromo-1,8-naphthalic anhydride, sodium azide and 4-amino-1-Boc-piperidine. The facile and economic synthesis is important for the wide use of such type of the dual-reactable probe. For control study, probe 2 was prepared by a five-step synthesis (see ESI). Probes 1–3 were well characterized by <sup>1</sup>H NMR, <sup>13</sup>C NMR and HRMS (see ESI).

The absorption spectra of the probes 1–3 were further examined for understanding the mechanism (Fig. 2). The dual-reactable probe 1 exhibited absorbance peaks at 365 nm and 506 nm, which were assigned to azide naphthalimide and NBD moieties, respectively. Upon treatment with H<sub>2</sub>S, a time-dependent decrease at 365 nm and an increase at 435 nm with an isosbestic point at 405 nm were observed (Fig. 2a), due to the reduction of azide to amine; because the control probe 3 exhibited the similar change with the same isosbestic point (Fig. 2c). The NBD absorbance for 1 or 2 in the presence of H<sub>2</sub>S displayed a decrease absorbance at around 500 nm and an increase at about 535 nm, respectively, due to thiolysis of NBD amine. The NBD-based probe 2 showed

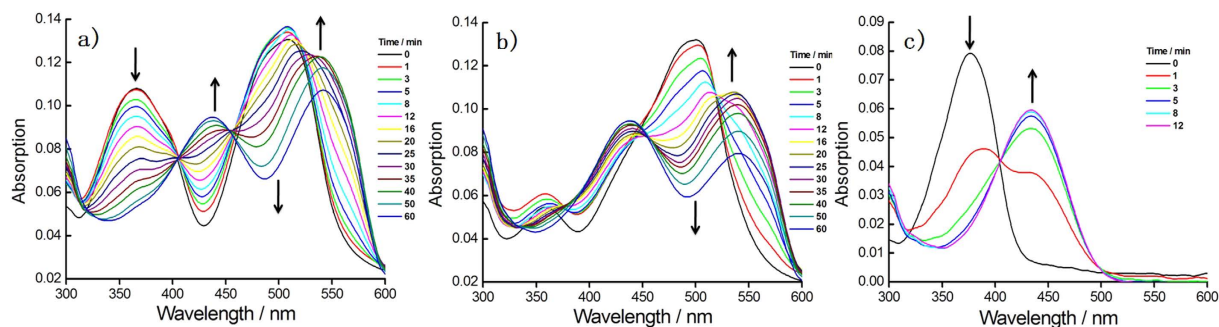


**Figure 2.** Absorption spectra revealed that probe 1 underwent both redox and nucleophilic reactions in the presence of  $\text{H}_2\text{S}$ . Time-dependent absorption spectra of 1 (a) or 2 (b) or 3 (c) in the presence of  $\text{H}_2\text{S}$ . Probes were  $10\ \mu\text{M}$ . For (a,b),  $\text{H}_2\text{S}$  were  $2\ \text{mM}$ ; for (c),  $\text{H}_2\text{S}$  was  $1\ \text{mM}$ .

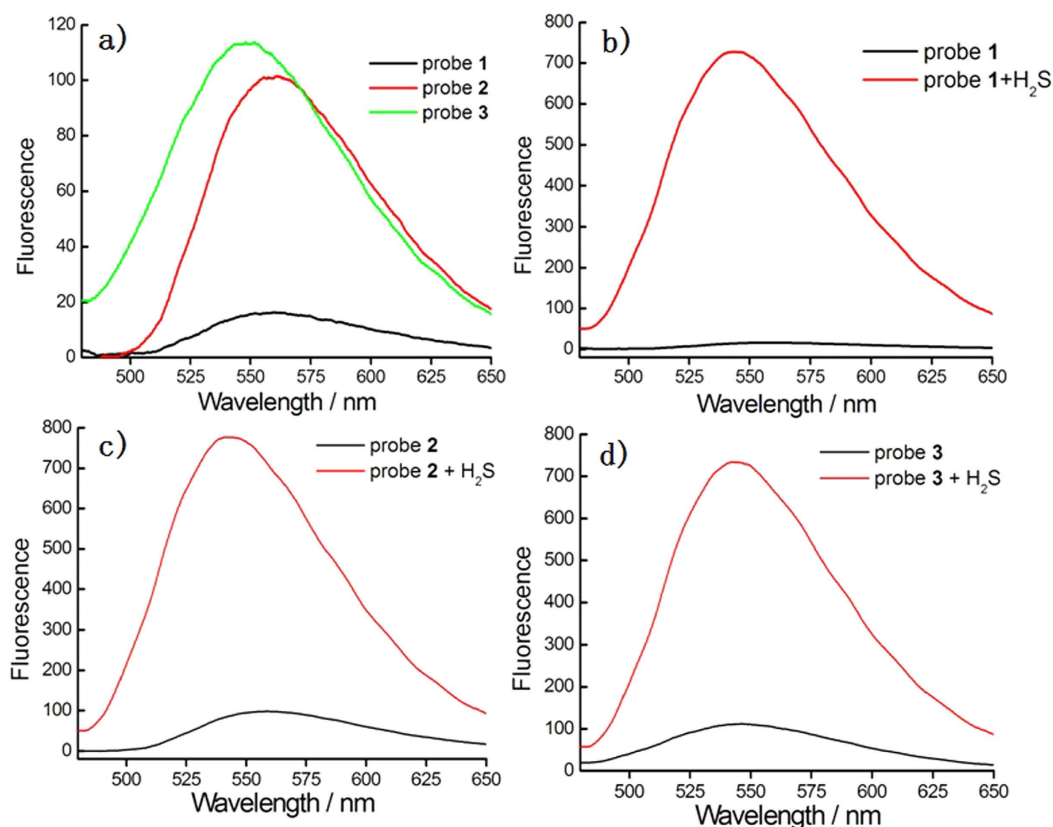


**Figure 3.** The dual-reactable probe 1 gave higher fluorescent turn-on response toward  $\text{H}_2\text{S}$  than that of single-reactable probes 2 and 3. (a) The fluorescence spectra of pure probes 1–3 ( $1\ \mu\text{M}$ ) upon excitation at  $425\ \text{nm}$  in PBS buffer (pH 7.4). (b) Fluorescence response of 1 ( $1\ \mu\text{M}$ ) toward  $\text{H}_2\text{S}$  ( $500\ \mu\text{M}$ ) for 60 min. (c) Fluorescence response of 2 ( $1\ \mu\text{M}$ ) toward  $\text{H}_2\text{S}$  ( $500\ \mu\text{M}$ ) for 60 min. (d) Fluorescence response of 3 ( $1\ \mu\text{M}$ ) toward  $\text{H}_2\text{S}$  ( $200\ \mu\text{M}$ ) for 30 min. Slits for all spectra:  $5/10\ \text{nm}$  (excitation/emission).

slower reaction rate toward  $\text{H}_2\text{S}$  than that of the azide-based probe 3 (Fig. S1), and the reaction kinetics of the dual-quenching probe 1 was mainly decided by the property of the relative slow reaction site. In summary, the absorption change of single-reactable probes toward  $\text{H}_2\text{S}$  showed similar response with that of the one-reactive site from the dual-reactable probe, implying that the dual-reactable probe could undergo two orthogonal reactions with  $\text{H}_2\text{S}$  simultaneously.

As shown in Fig. 3, emission spectra of probes 1–3 were checked in the absence or presence of  $\text{H}_2\text{S}$  in PBS (pH 7.4). As expected, the naphthalimide emission was heavily quenched for probe 1 due to FRET-ICT dual-quenching effects. While single-reactable probes 2 and 3 showed relative strong fluorescence under similar test conditions. These results implied that the combined usage of FRET-ICT dual-quenching effects is more efficient than that of any FRET or ICT single-quenching effect. After reacting with  $\text{H}_2\text{S}$ , the probe 1 showed

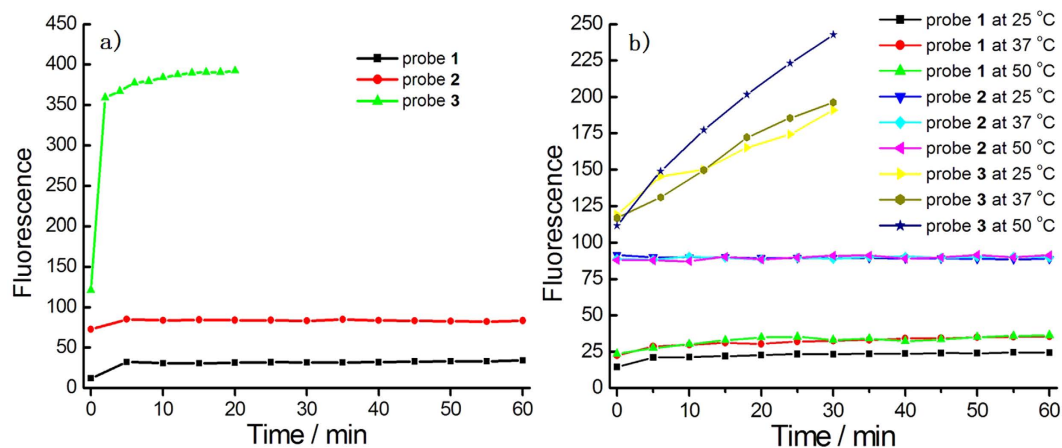


**Figure 4. Investigation of probes' stability by fluorescence.** Fluorescence intensity at 540 nm versus time of probes 1–3 (1  $\mu\text{M}$ ) in PBS buffer under a UV lamp (365 nm, 16 W) (a) or not (b).

significantly turn-on fluorescent response at 540 nm, with off-on response up to ca. 54.8 fold for **1**. The off-on response of **2** or **3** upon  $\text{H}_2\text{S}$  treatment was ca. 9.5 fold or 6.6 fold, either of which was much smaller than that of **1**, while the turn-on fold of **1** could be determined by multiplication of each turn-on fold of single-reactable probes **2** and **3**. Therefore, we can draw the conclusion that the fluorescence turn-on fold upon reacting with  $\text{H}_2\text{S}$  for dual-reactable probe is indeed greatly increased via dual-quenching effect.

In next tests, the dual- and single-reactable probes were incubated in PBS buffer for the thermo- and photo-stability tests (Fig. 4). The results indicated that the fluorescence increase of dual-reactable probe **1** was almost negligible even under UV light for 1 h, while the single-reactable azide-based probe showed an obvious fluorescent increase (Fig. 4a). Even without UV light, single-reactable probe **3** showed a certain fluorescent increase at different temperature while the dual-reactable probe **1** had much better stability (Fig. 4b). These results further indicated the advance of the dual-reactable probe.

A major challenge for  $\text{H}_2\text{S}$  detection in biological systems is to develop a selective probe that exhibits distinctive response to  $\text{H}_2\text{S}$  over millimolar biothiols and other reactive sulfur species. To design a highly selective  $\text{H}_2\text{S}$  probe, we used dual-reactable groups on one fluorophore; and the reactable group is also the quenching group. If a competitor can react with 10% probe in nucleophilic reaction site or with 20% in redox site, the maximal turn-on effect for a dual-reaction quenched fluorescent probe is only about 2% ( $10\% \times 20\%$ ). Such a dual-reactable strategy should increase the probe's selective response between  $\text{H}_2\text{S}$  and the competitor.

Probes **1–3** were incubated with various biological-related species in PBS and the maximal emission change was measured accordingly (Fig. 5 and S2). The tested species included biothiols (GSH, 5 mM; Cys, 1 mM; Hcy, 1 mM), reactive oxygen species ( $\text{H}_2\text{O}_2$ ,  $\text{ClO}^-$ ), reactive sulfur species ( $\text{SO}_4^{2-}$ ,  $\text{S}_2\text{O}_3^{2-}$ ,  $\text{SO}_3^{2-}$ ), anions ( $\text{NO}_2^-$ ,  $\text{N}_3^-$ ) and cations ( $\text{Zn}^{2+}$ ,  $\text{Fe}^{3+}$ ). For dual-reactable probe **1**, fluorescence intensity enhancement for any tested molecule in PBS (pH 7.4) was almost negligible except  $\text{H}_2\text{S}$ . While for single-reactable probes **2** and **3**,  $\text{SO}_3^{2-}$  or biothiols showed a certain fluorescence response. The dual-reactable probe **1** was further tested for its competitive selectivity over millimolar biothiols and  $\text{SO}_3^{2-}$  anion. The results indicated that probe **1** has higher selectivity than that of the single-reactable probes and is highly selective toward  $\text{H}_2\text{S}$  over other biologically relevant species. These results indicated that the selectivity of **1** could be determined by multiplication of selectivity of single-reactable probes **2** and **3**, which is indeed greatly improved via dual-reactable effect.

To obtain the detection limit for **1**, the fluorescence intensity change was closely monitored by addition of various concentrations of  $\text{H}_2\text{S}$  into the probe (Fig. S3a). The fluorescence intensity at 540 nm was linearly related to the concentrations of  $\text{H}_2\text{S}$  from 5 to 40  $\mu\text{M}$ , and the detection limit for **1** was calculated to be 0.9  $\mu\text{M}$  by using the  $3\sigma/k$  method<sup>12</sup>. The results implied that probe **1** is sensitive enough toward  $\text{H}_2\text{S}$  in buffer solution. The detection limit of probes **2** or **3** was determined to be 2.5  $\mu\text{M}$  or 2.6  $\mu\text{M}$ , respectively, which was lower than that of the dual-reactable probe **1** (Fig. S3). We also investigated the fluorescence response of probe **1** to  $\text{H}_2\text{S}$  under different pH values (Fig. S4). Results indicated that the probe **1** can function over a wide range of pH from 6.0 to 8.5, and the best response range is within pH 7.4–8.5. However, in the case of weak acidic conditions (pH < 7.0), the fluorescence turn-on signal is marginally lower, which was commonly observed in nucleophilic-reaction probes<sup>29–33</sup>.

To test the biological applicability of the dual-reactable probe **1**, we examined whether **1** can be used to detect exogenous  $\text{H}_2\text{S}$  in living cells (Fig. 6). HEK293A cells were treated with probe **1** and then washed with PBS to remove excess **1**. The **1**-loaded cells were incubated with  $\text{Na}_2\text{S}$  (50 or 200  $\mu\text{M}$ ) and subsequently imaged using a confocal fluorescence microscopy. The addition of both probe **1** and  $\text{H}_2\text{S}$  resulted in an obvious yellow fluorescence while the cells treated with only probe **1** did not show fluorescence. Merge images show that cells retained good morphology after incubation with **1** (Fig. 6), which suggested the good biocompatibility of **1**. The cytotoxicity of the probe **1** was further evaluated by MTT assay (Fig. S6), which did not show obvious cytotoxicity at 1–10  $\mu\text{M}$  range. These studies implied that **1** is cell-permeable and can image intracellular  $\text{H}_2\text{S}$  in living cells.

Finally, we compared the selectivity for bioimaging of dual-reactable probe **1** and its corresponding control probes **2** and **3** in living cells. Firstly, cells were treated with probes and then washed with PBS buffer to remove

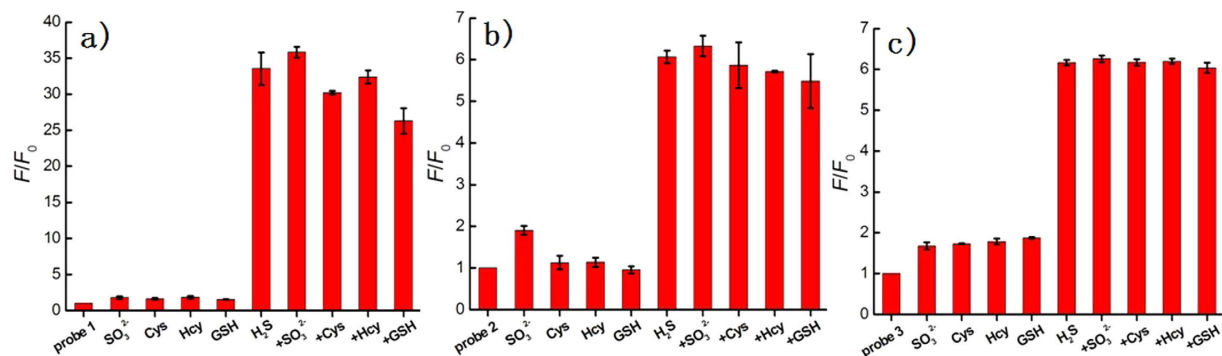


**Figure 5.** The dual-reactable probe **1** is more selective toward H<sub>2</sub>S than that of single-reactable probes **2** and **3**. Relative emission intensities at 540 nm (excitation at 425 nm) of probe **1** (a) or **2** (b) or **3** (c) in the presence of test species in PBS (pH 7.4). The test lanes: SO<sub>3</sub><sup>2-</sup> (200 μM), Cys (1 mM), Hcy (1 mM), GSH (5 mM), H<sub>2</sub>S (200 μM), H<sub>2</sub>S (200 μM) + SO<sub>3</sub><sup>2-</sup> (200 μM), H<sub>2</sub>S (200 μM) + Cys (1 mM), H<sub>2</sub>S (200 μM) + Hcy (1 mM), H<sub>2</sub>S (200 μM) + GSH (5 mM).

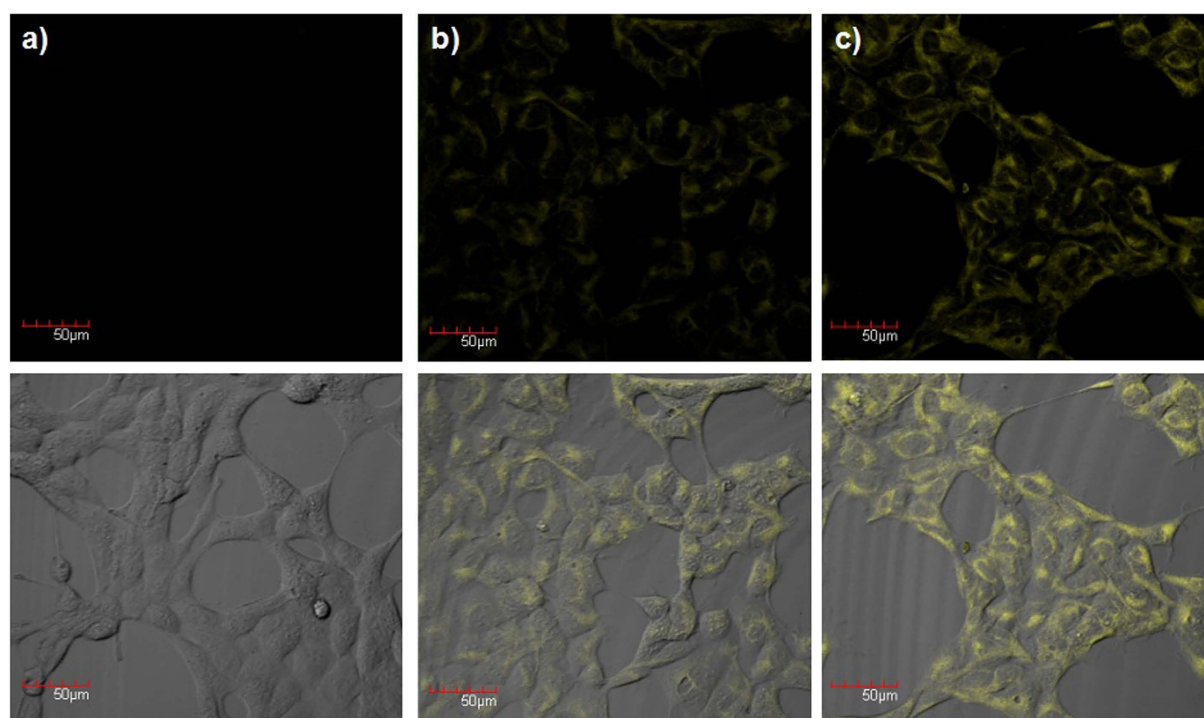


**Figure 6.** Confocal microscopy images of exogenous H<sub>2</sub>S in living cells using probe **1**. HEK293 cells were incubated with (a) **1** (5 μM) for 30 min, (b,c) **1** (5 μM) for 30 min, washed by PBS buffer, and then Na<sub>2</sub>S ((b) 50 μM; (c) 200 μM) for 60 min. The merge images between fluorescent and bright-field images are below. Scale bar, 50 μm.

excess probes. The selectivity experiments indicated that sulfite anions could react with both single-reactable probes **2** and **3**, and therefore sulfite anions were added in the probe-loaded cells. The time-dependent fluorescent images and intensities (Fig. 7 and S5) indicated that **1**-loaded cells kept instant fluorescence while **2**- and **3**-loaded cells showed increased fluorescence. These preliminary results implied that the dual-reactable probe **1** could be more selective in bioimaging than that of single-reactable probes **2** and **3**.

## Conclusion

A new redox-nucleophilic dual-reactable fluorescent probe based on naphthalimide as fluorophore was developed for H<sub>2</sub>S detection in aqueous buffer and in living cells, which showed higher selectivity, stability and fluorescent turn-on fold than that of single-reactable probes **2** and **3**. The “exact” control probes of **1** revealed that the improved turn-on fold and selectivity of the dual-reactable probe could be magnitude of multiplication from that of the two single-reactable probes **2** and **3**. Furthermore, the dual-reactable probe **1** could be successfully

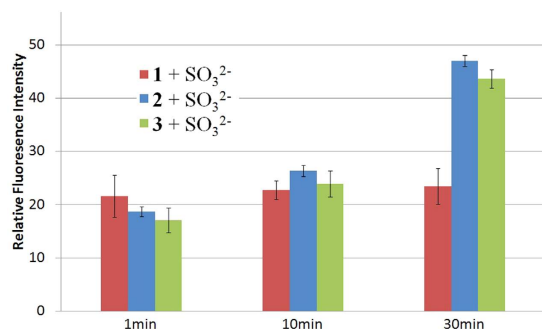


**Figure 7. The dual-reactable probe 1 is more selective than that of single-reactable probes 2 and 3 in bioimaging.** The average fluorescence of confocal microscopy images for probes 1–3 (5  $\mu$ M) after the addition of  $\text{SO}_3^{2-}$  anions (250  $\mu$ M) for 1 min, 10 min and 30 min.

used to image exogenous  $\text{H}_2\text{S}$  in living cells selectively and efficiently. Our results further imply that using such redox-nucleophilic dual-reactable strategy could be general for preparation of highly selective and sensitive  $\text{H}_2\text{S}$  probes for various biological applications.

## Methods

**Synthesis of 3.** 4-Azido-1,8-naphthalic anhydride<sup>24</sup> (4.83 g, 20.2 mmol) and 4-amino-1-Boc-piperidine (3.64 g, 18.2 mmol) were dissolved in ethanol (200 ml), the mixture was heated to reflux with stirring overnight. The reaction was monitored by TLC on pre-coated silica plates. After cooling down to room temperature, the reaction mixture was added with ice water to obtain a yellow precipitate, which was collected by vacuum filtration and washed with ice water. The resulting residue was subjected to column chromatography on silica (0.5% MeOH in  $\text{CH}_2\text{Cl}_2$ ), yielding a yellow solid **6** (2.6 g, 31%).  $R_f$  (5% MeOH in  $\text{CH}_2\text{Cl}_2$ ), 0.6.  $^1\text{H NMR}$  (400 MHz,  $\text{CDCl}_3$ )  $\delta$  8.57 (d,  $J = 7.3$  Hz, 1H), 8.52 (d,  $J = 8.0$  Hz, 1H), 8.38 (d,  $J = 8.4$  Hz, 1H), 7.74–7.68 (m, 1H), 7.43 (d,  $J = 8.0$  Hz, 1H), 5.21–5.09 (m, 1H), 4.29 (d,  $J = 26.9$  Hz, 2H), 2.84 (s, 2H), 2.78–2.66 (m, 2H), 1.66 (d,  $J = 12.7$  Hz, 2H), 1.48 (s, 9H);  $^{13}\text{C NMR}$  (101 MHz,  $\text{CDCl}_3$ )  $\delta$  164.4, 164.0, 154.8, 143.4, 132.3, 131.8, 129.2, 128.7, 127.0, 124.3, 123.0, 119.3, 114.8, 79.6, 77.5, 77.2, 76.8, 51.9, 28.6, 28.4. Probe **3** was obtained by treatment of **6** (960 mg, 2.3 mmol) with TFA: $\text{CH}_2\text{Cl}_2$  (1:1) solution at room temperature, which was removed under reduced pressure. The resulting residue was dissolved by ethyl acetate, distilled with saturated  $\text{NH}_4\text{Cl}$  solution and dried finally to obtain a yellow powder.  $^1\text{H NMR}$  (400 MHz,  $d_6$ -DMSO)  $\delta$  8.50 (d,  $J = 7.3$  Hz, 1H), 8.44 (d,  $J = 8.0$  Hz, 1H), 8.38 (d,  $J = 8.4$  Hz, 1H), 7.84 (t,  $J = 7.9$  Hz, 1H), 7.72 (d,  $J = 8.0$  Hz, 1H), 5.18–5.07 (m, 1H), 3.34 (d,  $J = 11.9$  Hz, 2H), 2.98 (t,  $J = 12.2$  Hz, 2H), 2.82–2.70 (m, 2H), 1.81 (d,  $J = 11.9$  Hz, 2H);  $^{13}\text{C NMR}$  (101 MHz,  $d_6$ -DMSO)  $\delta$  163.7, 163.2, 142.7, 131.7, 131.6, 128.4, 128.3, 127.4, 123.4, 122.5, 118.5, 116.0, 26.0. HRMS: calcd for  $[\text{M} + \text{H}]^+$ , 322.1299; found 322.1302.

**Synthesis of 1.** To a solution of **3** (290 mg, 0.9 mmol) and 4-chloro-7-nitrobenzofurazan (360 mg, 1.8 mmol) in 10 ml anhydrous DMF, DIPEA (618  $\mu$ l, 3.6 mmol) was added drop by drop. The reaction mixture was stirred at room temperature for 3 h and then poured into 120 ml ice water, which was distilled with  $\text{CH}_2\text{Cl}_2$  and dried. The resulting residue was subjected to column chromatography on silica (0.5% MeOH in  $\text{CH}_2\text{Cl}_2$ ), yielding a red solid **1** (414 mg, 95%).  $R_f$  (5% MeOH in  $\text{CH}_2\text{Cl}_2$ ), 0.6.  $^1\text{H NMR}$  (400 MHz,  $\text{CDCl}_3$ )  $\delta$  8.57 (d,  $J = 7.3$  Hz, 1H), 8.52 (d,  $J = 8.0$  Hz, 1H), 8.43 (d,  $J = 4.5$  Hz, 1H), 8.41 (d,  $J = 3.9$  Hz, 1H), 7.73 (t,  $J = 7.9$  Hz, 1H), 7.45 (d,  $J = 8.0$  Hz, 1H), 6.35 (d,  $J = 9.0$  Hz, 1H), 5.58–5.45 (m, 1H), 5.00 (d,  $J = 9.1$  Hz, 2H), 3.60 (t,  $J = 12.3$  Hz, 2H), 3.05–2.89 (m, 2H), 2.03 (d,  $J = 10.0$  Hz, 2H);  $^{13}\text{C NMR}$  (101 MHz,  $\text{CDCl}_3$ )  $\delta$  164.4, 164.0, 145.0, 145.0, 144.9, 143.9, 135.5, 132.6, 132.1, 129.2, 129.1, 127.1, 124.3, 123.1, 122.6, 118.8, 114.9, 102.6, 50.1, 49.9, 28.1. HRMS: calcd for  $[\text{M} + \text{H}]^+$ , 485.1316; found 485.1320.

**Procedure of fluorescence measurements.** Fluorescence studies were carried out using F-280 spectrophotometer (Tianjin Gangdong Sci & Tech., Development. Co., Ltd). 1–1000 mM Stock solutions of  $\text{Na}_2\text{S}$  in degassed PBS buffer were used as  $\text{H}_2\text{S}$  source. Probes were diluted in PBS buffer (pH = 7.4, 50 mM, 30% DMSO) to afford the final concentration of 1–10  $\mu$ M. For the selectivity experiment, different biologically relevant molecules (100 mM) were prepared as stock solutions in degassed PBS buffer. Appropriate amount of biologically relevant species were added to separate portions of the probe solution and mixed thoroughly. The reaction mixture was shaken uniformly before emission spectra were measured. For the time-course experiment, 1  $\mu$ M probe in PBS buffer were added with 500  $\mu$ M or 200  $\mu$ M  $\text{Na}_2\text{S}$  at room temperature, and the emission was measured at different time points. For the pH-dependent experiment, probe **1** (1  $\mu$ M) and  $\text{Na}_2\text{S}$  (200  $\mu$ M) were incubated with PBS buffers at different pH values. All measurements were performed in a 3 ml corvette with 2 ml solution.

**Cell culture and Bioimaging.** HEK-293 cells were cultured at 37  $^\circ\text{C}$ , 5%  $\text{CO}_2$  in DMEM/HIGH GLUCOSE (GIBCO) supplemented with 10% fetal bovine serum (FBS), 100 U/ml penicillin, 100  $\mu$ g/ml streptomycin, and 4 mM L-glutamine. The cells were maintained in exponential growth, and then seeded in glass-bottom 35 mm plate at the density about  $2 \times 10^4$ /well. Cells were passaged every 2–3 days and used

between passages 3 and 10. Cells were imaged on a confocal microscope (Olympus FV1000 UPLSAPO40X) with a 40 × objective lens. Emission was collected at yellow channel (500–600 nm) with 405 nm excitation. All images were analyzed with Olympus FV1000-ASW.

## References

1. Szabó, C. Hydrogen sulfide and its therapeutic potential. *Nat. Rev. Drug Discov.* **6**, 917–935 (2007).
2. Li, L., Rose, P. & Moore, P. K. Hydrogen sulfide and cell signaling. *Annu. Rev. Pharmacol. Toxicol.* **51**, 169–187 (2011).
3. Predmore, B. L., Lefter, D. J. & Gojon, G. Hydrogen Sulfide in Biochemistry and Medicine. *Antioxid. Redox Signaling.* **17**, 119–140 (2012).
4. Whiteman, M. & Moore, P. K. Hydrogen sulfide and the vasculature: a novel vasculoprotective entity and regulator of nitric oxide bioavailability? *J. Cell. Mol. Med.* **13**, 488–507 (2009).
5. Kimura, H. Hydrogen sulfide: its production and functions. *Exp. Physiol.* **96**, 833–835 (2011).
6. Yang, G. *et al.* H<sub>2</sub>S as a physiologic vasorelaxant: hypertension in mice with deletion of cystathionine  $\gamma$ -lyase. *Science* **322**, 587–590 (2008).
7. Kimura, H. Hydrogen sulfide: its production, release and functions. *Amino. Acides.* **41**, 113–121 (2011).
8. Fiorucci, S. *et al.* The third gas: H<sub>2</sub>S regulates perfusion pressure in both the isolated and perfused normal rat liver and in cirrhosis. *Hepatology.* **42**, 539–548 (2005).
9. Jiménez, D. *et al.* A new chromo-chemodosimeter selective for sulfide anion. *J. Am. Chem. Soc.* **125**, 9000–9001 (2003).
10. Searcy, D. G. & Peterson, M. A. Hydrogen sulfide consumption measured at low steady state concentrations using a sulfidostat. *Anal. Biochem.* **324**, 269–275 (2004).
11. Lawrence, N. S. *et al.* The electrochemical analog of the methylene blue reaction: a novel amperometric approach to the detection of hydrogen sulfide. *Electroanalysis.* **12**, 1453–1460 (2000).
12. Radford-Knoery, J. & Cutter, G. A. Determination of carbonyl sulfide and hydrogen sulfide species in natural waters using specialized collection procedures and gas chromatography with flame photometric detection. *Anal. Chem.* **65**, 976–982 (1993).
13. Lin, V. S. *et al.* Chemical probes for molecular imaging and detection of hydrogen sulfide and reactive sulfur species in biological systems. *Chem. Soc. Rev.* **44**, 4596–4618 (2015).
14. Yu, F. *et al.* Fluorescent probe for hydrogen sulfide detection and bioimaging. *Chem. Commun.* **50**, 12234–12249 (2014).
15. Lippert, A. R., New, E. J. & Chang, C. J. Reaction-based fluorescent probes for selective imaging of hydrogen sulfide in living cells. *J. Am. Chem. Soc.* **133**, 10078–10080 (2011).
16. Peng, H. *et al.* A fluorescent probe for fast and quantitative detection of hydrogen sulfide in blood. *Angew. Chem. Int. Ed.* **50**, 9672–9675 (2011).
17. Montoya, L. A. & Pluth, M. D. Selective turn-on fluorescent probes for imaging hydrogen sulfide in living cells. *Chem. Commun.* **48**, 4767–4769 (2012).
18. Chen, B. F. *et al.* Fluorescent probe for highly selective and sensitive detection of hydrogen sulfide in living cells and cardiac tissues. *Analyst.* **138**, 946–951 (2013).
19. Sun, W. *et al.* A two-photon fluorescent probe with near-infrared emission for hydrogen sulfide imaging in biosystems. *Chem. Commun.* **49**, 3890–3892 (2013).
20. Lin, V. S., Lippert, A. R. & Chang, C. J. Cell-trappable fluorescent probes for endogenous hydrogen sulfide signaling and imaging H<sub>2</sub>O<sub>2</sub>-dependent H<sub>2</sub>S production. *Proc. Natl. Acad. Sci. USA* **110**, 7131–7135 (2013).
21. Zhou, G. D. *et al.* An NBD fluorophore-based colorimetric and fluorescent chemosensor for hydrogen sulfide and its application for bioimaging. *Tetrahedron* **69**, 867–870 (2013).
22. Wei, L. *et al.* FRET ratiometric probes reveal the chiral sensitive cysteine-dependent H<sub>2</sub>S production and regulation in living cells. *Sci. Rep.* **4**, 4521 (2014).
23. Henthorn, H. A. & Pluth, M. D. Mechanistic insights into the H<sub>2</sub>S-mediated reduction of aryl azides commonly used in H<sub>2</sub>S detection. *J. Am. Chem. Soc.* **137**, 15330–15336 (2015).
24. He, L. W. *et al.* A new strategy to construct a FRET platform for ratiometric sensing of hydrogen sulfide. *Chem. Commun.* **51**, 1510–1513 (2015).
25. Yu, F. *et al.* An ICT-based strategy to a colorimetric and ratiometric fluorescence probe for hydrogen sulfide in living cells. *Chem. Commun.* **48**, 2852–2854 (2012).
26. Wan, Q. Q. *et al.* *In vivo* monitoring of hydrogen sulfide using a cresyl violet-based ratiometric fluorescence probe. *Chem. Commun.* **49**, 502–504 (2013).
27. Bae, S. K. *et al.* A ratiometric two-photon fluorescent probe reveals reduction in mitochondrial H<sub>2</sub>S production in Parkinson's disease gene knockout astrocytes. *J. Am. Chem. Soc.* **135**, 9915–9923 (2013).
28. Zhang, L. *et al.* A colorimetric and ratiometric fluorescent probe for the imaging of endogenous hydrogen sulphide in living cells and sulphide determination in mouse hippocampus. *Org. Biomol. Chem.* **12**, 5115–5125 (2014).
29. Cao, X. W. *et al.* A near-infrared fluorescent turn-on probe for fluorescence imaging of hydrogen sulfide in living cells based on thiolysis of dinitrophenyl ether. *Chem. Commun.* **48**, 10529–10531 (2012).
30. Wei, C. *et al.* NBD-based colorimetric and fluorescent turn-on probes for hydrogen sulfide. *Org. Biomol. Chem.* **12**, 479–485 (2014).
31. Wei, C., Wei, L., Xi, Z. & Yi, L. A FRET-based fluorescent probe for imaging H<sub>2</sub>S in living cells. *Tetrahedron Lett.* **54**, 6937–6939 (2013).
32. Chen, Y. *et al.* A ratiometric fluorescent probe for rapid detection of hydrogen sulfide in mitochondria. *Angew. Chem. Int. Ed.* **52**, 1688–1691 (2013).
33. Zhang L. *et al.* A highly selective and sensitive near-infrared fluorescent probe for imaging of hydrogen sulphide in living cells and mice. *Sci. Rep.* **6**, 18868 (2016).
34. Qian, Y. *et al.* Selective fluorescent probes for live-cell monitoring of sulphide. *Nat. Commun.* **2**, 495 (2011).
35. Liu, C. R. *et al.* Capture and visualization of hydrogen sulfide by a fluorescent probe. *Angew. Chem. Int. Ed.* **50**, 10327–10329 (2011).
36. Xu, Z. *et al.* A highly selective fluorescent probe for fast detection of hydrogen sulfide in aqueous solution and living cells. *Chem. Commun.* **48**, 10871–10873 (2012).
37. Qian, Y. *et al.* A fluorescent probe for rapid detection of hydrogen sulfide in blood plasma and brain tissues in mice. *Chem. Sci.* **3**, 2920–2923 (2012).
38. Wang, X. *et al.* A near-infrared ratiometric fluorescent probe for rapid and highly sensitive imaging of endogenous hydrogen sulfide in living cells. *Chem. Sci.* **4**, 2551–2556 (2013).
39. Huang, Z. J. *et al.* Aldehyde group assisted thiolysis of dinitrophenyl ether: a new promising approach for efficient hydrogen sulfide probes. *Chem. Commun.* **50**, 9185–9187 (2014).
40. Zhang, H. T. *et al.* A highly selective and sensitive fluorescent thiol probe through dual-reactive and dual-quenching groups. *Chem. Commun.* **51**, 2029–2032 (2015).
41. Zhang, C. Y. *et al.* A FRET-ICT dual-quenching fluorescent probe with large off-on response for H<sub>2</sub>S: synthesis, spectra and bioimaging. *Chem. Commun.* **51**, 7505–7508 (2015).
42. Wei, C. *et al.* Dual-Reactable fluorescent probes for highly selective and sensitive detection of biological H<sub>2</sub>S. *Chem. Asian J.*, doi: 10.1002/asia.201600262 (2016).
43. Long, G. L. & Winefordner, J. D. Limit of detection a closer look at the IUPAC definition. *Anal. Chem.* **55**, 712A–724A (1983).

## Acknowledgements

This work was supported by the MOST (2010CB126102), NSFC (21332004, 21402007) and the Fundamental Research Funds for the Central Universities (YS1401).

## Author Contributions

L.Y. and Z.X. conceived the idea and directed the work. C.Z., L.C. and B.L. performed the organic synthesis and characterizations. R.W. performed the cell-based imaging. All authors contributed to data analysis and manuscript writing.

## Additional Information

**Supplementary information** accompanies this paper at <http://www.nature.com/srep>

**Competing financial interests:** The authors declare no competing financial interests.

**How to cite this article:** Zhang, C. *et al.* A Redox-Nucleophilic Dual-Reactable Probe for Highly Selective and Sensitive Detection of H<sub>2</sub>S: Synthesis, Spectra and Bioimaging. *Sci. Rep.* **6**, 30148; doi: 10.1038/srep30148 (2016).



This work is licensed under a Creative Commons Attribution 4.0 International License. The images or other third party material in this article are included in the article's Creative Commons license, unless indicated otherwise in the credit line; if the material is not included under the Creative Commons license, users will need to obtain permission from the license holder to reproduce the material. To view a copy of this license, visit <http://creativecommons.org/licenses/by/4.0/>